Advances in Computer Science Research, volume 88

International Conference on Computer, Network, Communication and Information Systems (CNCI 2019)

High Precision and Pose Estimation Based on Improved Point Cloud Algorithm for Noncooperative Targets

Liang Wei[1, a], Jia Liu[2, b], Guiyang Zhang[3, c] and Ju Huo[1, d,*]

[1]School of Electrical Engineering and Automation, Harbin Institute of Technology, Harbin, China;

[2]Systems Engineering Research Institute, Beijing, China;

[3]School of Astronautics, Harbin Institute of Technology, Harbin, China;

[a]935295997@qq.com, [b]liujia02416@163.com, [c]dr_gyzhang@outlook.com, [d]torch@hit.edu.cn

Abstract. Aiming at protecting the space environment such as removing space debris and repairing malfunctioning targets, it is vital importance to measure the pose of space targets. In this paper we propose a high precision pose estimation algorithm based on point cloud. The optimized Random Sample Consensus (RANSAC) algorithm which applies iterative solution can effectively delete false matching points. The experiment system consists of a satellite model and a binocular camera. The proposed method is a vital part of new autonomous spacecraft measurement which only use a binocular camera system at different perspectives to complete the pose estimation. After obtaining the cloud data of a target, we use the improved crust algorithm to accomplish the three-dimensional model. Finally, the experiment has shown that the vision based method can obtain the pose information of the targets effectively.

Keywords: Binocular vision, RANSAC, pose estimation, crust, noncooperative target.

1. Introduction

Computer vision [1,2] is one of the significant means in 3D targets reconstruction. Compared to other measurement methods, it has the advantages of noncontact and high-precision [3-5]. Over the past decades, more and more spacecrafts have been launched into space every year, however, some abandoned objects which are out of control affect the safety of the space environment seriously. Therefore, estimate the position of space targets to keep the space environment clean becomes broad consensus. Noncooperative targets refer to the satellites or rockets which cannot communicate with other spacecrafts so that we have no way to learn their information such as motion and size. The abandoned rockets and the debris of satellites are all belong to these targets that have a strong impact on other operational crafts. In other words, if we cannot remove these space debris effectively, the normal working satellites may collide with the debris. On the other hand, the noncooperative targets have less prior information. All these disadvantages make it is difficulty to estimate the pose measurement of complex and unknown space targets.

A high-speed pose estimation method based on binocular vision theory was come up with W. Liu, et [6]. In this method, Liu used two high-speed CCD cameras to solve the problem of estimating scroll targets. J. Peng [7] introduced the vision-based measurement which is widely applied in the field of measurement by identifying the circular or near-circular shapes on the targets. For the purpose of eliminating the inaccurate survey of circular targets, C. Meng et [8] presented a new approach called perspective circle and line. But in practical applications, it is easily influenced by many factors such as the accuracy of camera calibration and the effect of features extraction. Different from other algorithms, if we know the structure of space targets, we can evaluate the pose without marking specifically [9]. Concerning the large uncontrolled satellites, X. Du et [10] applied two collaborative cameras to determine the pose estimation. G. Dong et [11] studied the calibration by means of using extended kalman filter. This algorithm has increased the processing speed via utilizing a single camera. Additionally, K. Klionovska [12] pointed out a model-based method to conduct the pose. T. Tzschichholz [13] made full use of fusing the data streams to design the location information.

All of the above studies have made a significant contribution to the pose estimation of space targets. The vision-based method has been widely researched due to its simple structure and low cost. In this paper, we will put forward a scheme by exploiting the binocular camera system. The section of this paper is organized as follows. Section 2 introduces an approach for extracting invariant features from images. In Section 3, the improved point cloud algorithm is proposed. In Section 4, the experiments are used to certify the feasibility of the proposed algorithm. At last, the conclusion is made in Section 5.

2. Detection of Feature Points

2.1 SIFT Algorithm.

The Scale Invariant Feature Transform (SIFT) method has strong matching ability to extract distinctive features such as invariant points which are unaffected by level shift, rotation and affine transform etc. Nowadays, SIFT algorithm is always used for detecting local features.

The Gaussian scale space is produced from the convolution of the image with variable-scale Gaussian kernels.

$$L(x,y,\sigma) = G(x,y,\sigma) * I(x,y) \tag{1}$$

$$G(x,y,\sigma) = \frac{1}{2\pi\sigma^2} e^{-\frac{\left(x-\frac{m}{2}\right)^2+\left(y-\frac{n}{2}\right)^2}{2\sigma^2}} \tag{2}$$

For the purpose of calculating feature points in scale space, we use the difference-of-Gaussian function to detect the extreme.

$$\begin{aligned} D(x,y,\sigma) &= \left(G(x,y,k\sigma) - G(x,y,\sigma)\right) * I(x,y) \\ &= L(x,y,k\sigma) - L(x,y,\sigma) \end{aligned} \tag{3}$$

After the above work, select candidate key points of those which has maximum or minimum pixel compared to its neighborhood and then use Hessian matrix to eliminate the edge points and low contrast points.

$$\begin{aligned} Tr(\boldsymbol{H}) &= D_{xx} + D_{yy} = \alpha+\beta \\ \mathrm{Det}(\boldsymbol{H}) &= D_{xx}D_{yy} - (D_{xy})^2 = \alpha\beta \end{aligned} \tag{4}$$

Then, we endow every feature point with a main gradient amplitude and direction.

$$\begin{aligned} m(x,y) &= \sqrt{\left(L(x+1,y)-L(x-1,y)\right)^2 + \left(L(x,y+1)-L(x,y-1)\right)^2} \\ \theta(x,y) &= \arctan\frac{\left(L(x,y+1)-L(x,y-1)\right)}{\left(L(x+1,y)-L(x-1,y)\right)} \end{aligned} \tag{5}$$

At last, use a 128 dimensional vector to describe each key point through calculating the gradient magnitude and orientation in the vicinity of the feature point. To avoid the change of illumination, feature vectors required to be normalized.

2.2 SURF Algorithm.

Compared with SIFT, the Speeded Up Robust Feature (SURF) is faster and gains better robustness in feature extraction.

Based on the integral image, SURF denotes box filter to approximate second order Gaussian derivatives and use D_{xx}, D_{yy} and D_{xy} to approximate the convolution result, then detect interest points based on Hessian matrix.

$$H(x,\sigma) = \begin{bmatrix} L_{xx}(x,\sigma) & L_{xy}(x,\sigma) \\ L_{xy}(x,\sigma) & L_{yy}(x,\sigma) \end{bmatrix} \tag{6}$$

$$Det(H) = D_{xx}D_{yy} - (\omega D_{xy})^2 \tag{7}$$

After the above work, the tri-linear interpolation method is used to obtain the subpixel level points and remove those interests which the value of Hessian matrix is less than a certain threshold. In order to obtain rotational invariance, SURF uses the Haar wavelet to calculate the responses in the circle area and define the direction of the longest vector as the main direction.

At last, create a square window and divide it into 16 areas which is centered on every key point. We apply the arithmetic weighted algorithm to compute the Haar wavelet value in the direction of x and y. Therefore each interest point can be represented by a 64 dimensional feature vector.

After getting the feature vectors from SIFT or SURF, take the euclidean distance between feature vectors to measure the similarity of two pictures obtained by binocular camera system. However, it is inefficient to judge the matching points by exhaustive method, we can use BBF algorithm based on the K-dimensional Tree (KD tree) to find KNN (K-nearest Neighbor) effectively. Choose a image and construct the KD tree according to its features. Find the nearest and the second nearest distance of every feature in another image. By calculating the scale of minimum distance and the minor minimum distance to determine if the match is correct.

3. Iterative Algorithm of Pose Estimation

3.1 Improved Pose Estimation Algorithm.

When we use euclidean distance to define simple registration, it may generate some false matching. We can use Random Sample Consensus (RANSAC) algorithm to solve the mismatches. Through by estimating a mathematical model form the original points obtained by BBF method, we get the best initial homography matrix. The detailed steps are shown below:

Choose four pairs from the matched points randomly and then use these points to calculate the matrix H.

$$\begin{bmatrix} u \\ v \\ 1 \end{bmatrix} = H \begin{bmatrix} u' \\ v' \\ 1 \end{bmatrix} \tag{8}$$

Repeat the above steps and record the number of inner points. If the number of inner points computed by H are more than the previous H, the current H is chosen as the best model.

$$\left\| \begin{bmatrix} x' \\ y' \\ 1 \end{bmatrix} - H \begin{bmatrix} x \\ y \\ 1 \end{bmatrix} \right\| \le t \tag{9}$$

Aiming at improving the registration efficiency, we use the improved [14] RANSAC based on the principle of approximate slope to calculated the homography matrix. Compared to the previous algorithm, we need to calculate the slope between the rough matching points obtained by SIFT or SURF and compute the homography matrix based on those matching points with similar slopes.

After use the RANSAC algorithm, we get the initially aligned point cloud. In order to estimate the pose accurately, we need to complete the surface reconstruction. So, we apply the advanced crust algorithm to complete precise alignment of 3D point cloud data [15]. After that, the spatial pose of targets can be displayed.

Crust algorithm is a three-dimensional reconstruction method which is based on Voronoi diagrams and Delaunay triangulations. Its core idea is to input a point cloud data and then get the central axis. Next, obtain the surface through converting the center axis. Finally, the point cloud model is rebuilt. The improved crust algorithm is shown as follows:

Create a boundary crust for point cloud and compute Voronoi diagram of sample points, the bounding box points are also considered as sample points. Find the poles of Voronoi vertices to build the Delaunay triangulation of point cloud containing poles and eliminate triangles that do not belong

inside the boundary. The cross coefficients are used to determine whether the tetrahedrons are in or out of the boundary. At last, extract boundary tetrahedrons to form the grid entity. Where If is the crossover coefficients, c_{i1}, c_{i2} are the centers of two adjacent tetrahedrons, r_{i1}, r_{i2} represent the radius the tetrahedrons.

$$If = (-|c_{i1} - c_{i2}|^2 + r_{i1}^2 + r_{i2}^2) / 2r_{i1}r_{i2} \tag{10}$$

3.2 Algorithm Analysis.

The binocular camera system is used to sample at different viewing angles. Detect the feature points by SIFT or SURF algorithm and use the ratio of euclidean distance to match the associated points. The improved RANSAC algorithm based on the slope can be applied to compute the matrix H. Through multiple iterations, we obtain the aligned point cloud on the basis of the best matrix H. According to the principle of binocular vision measurement, we calculate the 3d coordinates of feature points. Use a set of points contain Voronoi vertices and poles to form a rough triangular mesh. After applying the theory of Delaunay triangulation, we create the correspondence between tetrahedrons and triangles. The center coordinates of each tetrahedron were solved by the Cramer's rule and calculate the crossover coefficients of two tetrahedrons to identify the boundary tetrahedron. Finally, the completed and high-precision triangular grid was formed.

4. Experimental Results and Analyses

The proposed algorithm is implemented by VS2010 and verified on a computer with a 4.0 GHz CPU and 4 GB memory. The parameters of the binocular cameras in the simulation environment are as follows: Image resolution is 1280×1024 pixels, cell size is $du \times dv = 7.4 \times 7.4\ \mu m^2$. Fig. 1 shows the experimental facility and the measuring coordinate system.

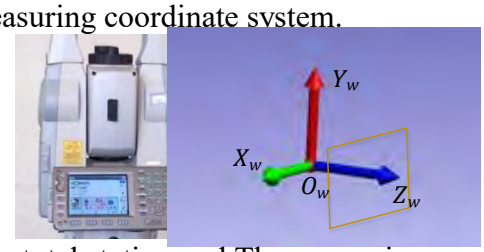

Fig. 1 Electronic total station and The measuring coordinate system

In this paper, we use the satellite model to simulate noncooperative target. Fig. 2(a) and (b) show the pictures of satellite taken at different angles. In order to verify the reliability of the algorithm, we change the lighting conditions and focal lengths. Fig. 3(a) and (b) describe the renders of feature points extracted by SIFT algorithm. The green cross indicates the location in pictures. In these two figures, we can see the SIFT algorithm can almost detect all the interest points.

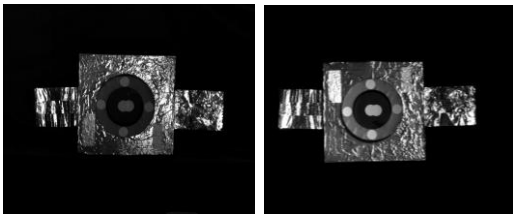

(a) (b)

Fig. 2 Pictures of satellite taken at different angles

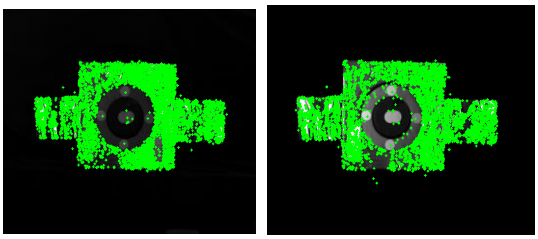

(a) (b)

Fig. 3 Pictures of satellite taken at different angles

We pick out the nearest and the second-nearest neighbor by using BBF algorithm based on KD-tree and define the value of threshold equal to 0.8. Fig. 4 shows the matching effect.

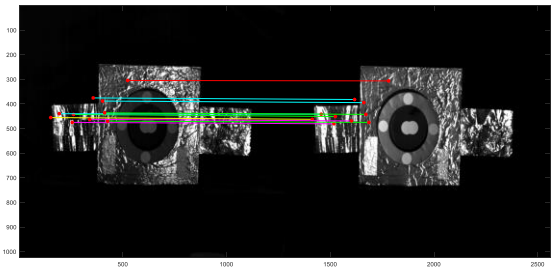

Fig. 4 Matching effect by using SIFT method

In this figure, we conclude that even though the SIFT algorithm can extract all the key points, the matching effect is terrible. Most feature points are not matched. So, we decided to use SURF method to identify the usefulness of this algorithm. Fig. 5(a) and (b) show vector diagrams which are generated by SURF algorithm. Fig. 6 describes the matching effect.

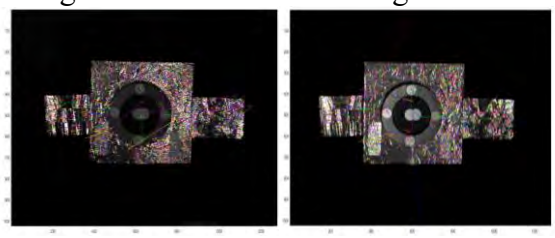

(a) (b)

Fig.5 Vector diagrams of two images

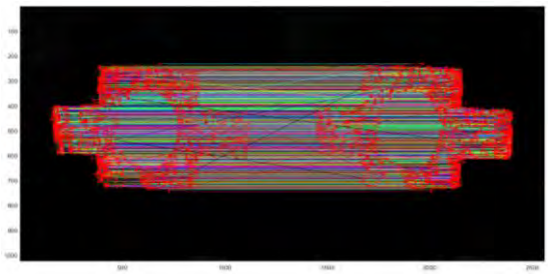

Fig. 6 Matching effect by using SURF method.

It can be found that the SURF algorithm has high accuracy and nearly all of the interest points can be initially matched. However, there are still generate some mismatches. In order to eliminate the mismatched points, we plan to use the improved RANSAC algorithm. The optimized matching effect can be seen in Fig. 7.

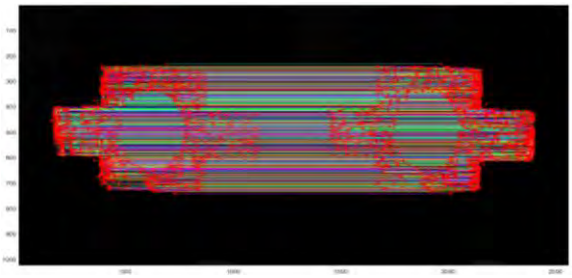

Fig. 7 Matching effect after using RANSAC method.

Fig. 8 displays the status of point cloud. On this basis, the advanced crust algorithm is implemented to reconstruct the three-dimensional model, as shown in Fig. 9.

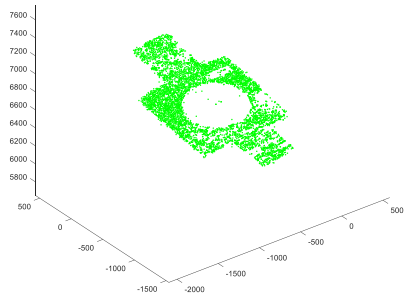

Fig. 8 Picture of target point cloud

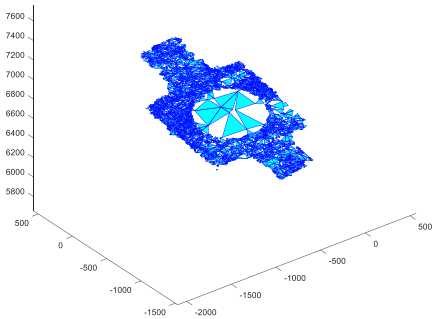

Fig. 9 Three-dimensional model

Compered to SIFT, the SURF algorithm can describe the corner points in detail. After utilizing the improved RANSAC theory, the 3D model can complete the estimation.

5. Conclusions

This paper is focus on addressing a high precision algorithm for position and attitude measurement of noncooperative targets. The optimized point cloud algorithm has achieved better measurement results. Compared with the original estimation algorithm, the proposed method has advantages in efficiency and accuracy which can be able to adapt the complex and variable space environment. The practical experiments are carried out to prove the feasibility of the algorithm. In addition, this research has become an important means of capturing mission to spatial noncooperative targets and space garbage clean up.

Acknowledgements

This work was supported in part by the National Science Foundation (NSFC) 61473100.

References

[1]. N. Naik, S.D.Kominers and R. Raskar, “Computer vision uncovers predictors of physical urban change,” P. Natl. A. Sci, vol. 114, pp. 7571-7576, 2017.

[2]. C. Kanellakis, G. Nikolakopoulos, “Survey on computer vision for UAVs: current developments and trends,” J. Intell. Robot. Syst, vol. 87, pp. 141-168, 2017.

[3]. H. B. Duan, H. Li and Q. Luo, “A binocular vision-based UAVs autonomous aerial refueling platform,” Sci. Chin. Inform. Sci, vol. 59, pp. 1-7, 2016.

[4]. J. Huo, G. Y. Zhang, and M. Yang, “Algorithm for pose estimation based on objective function with uncertainty-weighted measuring error of feature point cling to the curved surface,” Appl. Optics, vol. 57, pp. 3306–3315, 2018.

[5]. S. X. Tian, S. Lu and Z. M. Liu, “Levenberg-Marquardt algorithm based nonlinear optimization of camera calibration for relative measurement,” CCC, pp. 4868-4872, 2015.

[6]. W. Liu, X. Ma and Z. Y. Jia, “Position and attitude measurement of high-speed isolates for hypersonic facilities,” Measurement, vol. 62, pp. 63–73, 2015.

[7]. J. Q. Peng, W. F. Xu, H. Yuan, An efficient pose measurement method of a space non-cooperative target based on stereo vision, IEEE Access, 5: 22344-22362, 2017.

[8]. C. Meng, Z. X. Li and H. Sun, “Satellite pose estimation via single perspective circle and line,” IEEE. T. Aero. Elec. Sys, vol. 54, pp. 3084-3095, 2018.

[9]. S. J. Zhang, X. B. Cao, and M. Chen, “Monocular vision-based relative pose parameters determination for non-cooperative spacecrafts,” J. Nanjing Univ. Sci. Tech, 2006.

[10]. X. D. Du, B. Liang and W. F. Xu, “Pose measurement of large non-cooperative satellite based on collaborative cameras,” Acta. Astronaut, 2011.

[11]. G. Q. Dong, Z. H. Zhu, “Vision-based pose and motion estimation of non-cooperative target for space robotic manipulators,” AIAA Space Conf. Exp, 2014.

[12]. K. Klionovska, H. Benninghoff, “Initial pose estimation using PMD sensor during the rendezvous phase in on-orbit servicing missions,” AAS/AIAA Space Flight Mech. Meeting, 2017.

[13]. T. Tzschichholz, T. Boge and K. Schilling, “Relative pose estimation of satellites using PMD-/CCD-sensor data fusion,” Acta. Astronaut, vol. 109, pp. 25-33, 2015.

[14]. W. X. Jia, G. C. Zhang and L. L. Wang, “Image registration algorithm based on SIFT and improved RANSAC,” Comput. Eng. Appl, vlo. 54, pp. 203-207, 2018.

[15]. Z. Chen, J. Wang, “Automatic modeling of point cloud grid with improved Crust algorithm,” Sci. Surveying Mapping, 2018.